Published in final edited form as:

Antiviral Res. 2017 November ; 147: 91–99. doi:10.1016/j.antiviral.2017.10.008.

Identification of 2′-deoxy-2′-fluorocytidine as a potent inhibitor of Crimean-Congo hemorrhagic fever virus replication using a recombinant fluorescent reporter virus

Stephen R. Welch, **Florine E.M. Scholte**, **Mike Flint**, **Payel Chatterjee**, **Stuart T. Nichol**, **Éric Bergeron**, **Christina F. Spiropoulou***

Viral Special Pathogens Branch, Division of High-Consequence Pathogens and Pathology, National Center for Emerging and Zoonotic Infectious Diseases, Centers for Disease Control and Prevention, 1600 Clifton Road, MS G-14, Atlanta, GA, 30329, USA

Abstract

Crimean-Congo hemorrhagic fever virus (CCHFV), a tick-borne orthonairovirus, causes a severe hemorrhagic disease in humans (Crimean-Congo hemorrhagic fever, CCHF). Currently, no vaccines are approved to prevent CCHF; treatment is limited to supportive care and the use of ribavirin, the therapeutic benefits of which remain unclear. CCHF is part of WHO's priority list of infectious diseases warranting further research and development. To aid in the identification of new antiviral compounds, we generated a recombinant CCHFV expressing a reporter protein, allowing us to quantify virus inhibition by measuring the reduction in fluorescence in infected cells treated with candidate compounds. The screening assay was readily adaptable to high-throughput screening (HTS) of compounds using Huh7 cells, with a signal-to-noise ratio of 50:1, and Z′-factors > 0.6 in both 96- and 384-well formats. A screen of candidate nucleoside analog compounds identified 2′-deoxy-2′-fluorocytidine (EC_{50} = 61 ± 18 nM) as having 200 × the potency of ribavirin (EC_{50} = 12.5 ± 2.6 μM), as well as 17 × the potency of T-705 (favipiravir), another compound with reported anti-CCHFV activity (EC_{50} = 1.03 ± 0.16 μM). Furthermore, we also determined that 2′-deoxy-2′-fluorocytidine acts synergistically with T-705 to inhibit CCHFV replication without causing cytotoxicity. The incorporation of this reporter virus into the high-throughput screening assay described here will allow more rapid identification of effective therapeutic options to combat this emerging human pathogen.

1. Introduction

Crimean-Congo hemorrhagic fever (CCHF), a tick-borne disease in humans, is caused by CCHF virus (CCHFV), a tri-segmented, negative-sense RNA virus (genus *Orthonairovirus*, family *Nairoviridae*) (Kuhn et al., 2016). Its 3 genome segments are termed large (L), medium (M), and small (S) based on their relative lengths, and encode 3 genes: the RNA-dependent RNA-polymerase (RdRp), the glycoprotein precursor (GPC), and the nucleoprotein (NP), respectively (Zivcec et al., 2016). In humans, CCHF can range from a

*Corresponding author. ccs8@cdc.gov (C.F. Spiropoulou).

Appendix A. Supplementary data

Supplementary data related to this article can be found at http://dx.doi.org/10.1016/j.antiviral.2017.10.008.

non-specific mild febrile illness to hemorrhage, liver dysfunction, shock, and multi-organ failure in severe or fatal cases (Bente et al., 2013). CCHF case fatality rates vary widely, with estimates ranging from 5 to 30%, although rates of 50–80% have been reported during epidemic events (Dokuzoguz et al., 2013; Hoogstraal, 1979; Humolli et al., 2010; Mishra et al., 2011).

No licensed antiviral drugs or vaccines are currently available for CCHF. Treatment options remain largely supportive. Use of the broad-spectrum antiviral drug ribavirin is common; however, while several studies have suggested clinical benefits if ribavirin is administered early in infection (Dokuzoguz et al., 2013; Ozbey et al., 2014; Tasdelen Fisgin et al., 2009), others have reported no effect on mortality rates (Ascioglu et al., 2011; Köksal et al., 2010; Leblebicioglu et al., 2016; Soares-Weiser et al., 2010). T-705 (favipiravir) has recently shown higher efficacy than ribavirin in a mouse model of CCHF, but has not been used in human cases (Oestereich et al., 2016). The lack of treatment options, coupled with the recent WHO inclusion of CCHFV on a list of emerging pathogens likely to cause severe outbreaks in the near future, emphasizes the urgency for developing high-throughput screening methods to identify novel CCHF therapeutics (WHO, 2016).

Potential antiviral compounds can be screened *in vitro* by assessing reduction in viral protein expression via immunofluorescence, differences in virus-induced cell death, or changes in viral titers. However, these methods are often time-consuming, costly, and difficult to adapt for high-throughput screening assays. These limitations are further compounded by the requirement for biosafety level-4 (BSL-4) handling of CCHFV. To streamline the process of antiviral drug discovery, we developed a high-throughput screening assay for CCHFV using recombinant reporter CCHFV encoding the fluorescent protein ZsGreen1 (ZsG). Here, we demonstrate that this reporter virus allows rapid assessment of antiviral activity, and is amenable for high-throughput screening under BSL-4 conditions. A screen of nucleoside analogs identified 2′-deoxy-2′-fluorocytidine (2′-dFC) as a potential CCHFV antiviral, with greater potency than either ribavirin or T-705. Furthermore, the assay allowed rapid evaluation of the synergistic potential of candidate compounds, showing that 2′-dFC acts synergistically with T-705 to increase the potency of both compounds.

2. Materials and methods

2.1. Cells

Huh7 cells were cultured in Dulbecco’s modified Eagle’s medium (DMEM) supplemented with 5% (v/v) fetal calf serum (FCS), non-essential amino acids (NEAA), 100 U/mL penicillin, and 100 μg/mL streptomycin. SW13 and BSR-T7/5 cells were cultured in DMEM supplemented with 10% (v/v) FCS, NEAA, 1 mM sodium pyruvate, 2 mM L-glutamine, 100 U/mL penicillin, and 100 μg/mL streptomycin. HAP1 cells (Horizon Discovery) were cultured in Iscove’s modified Dulbecco’s medium supplemented with 10% FCS, 100 U/mL penicillin, and 100 μg/mL streptomycin.

2.2. Rescue of recombinant viruses

Recombinant infectious CCHFV was generated using a previously described reverse genetics system (Bergeron et al., 2015). Briefly, T7 promoter-based plasmids containing full-length anti-genomic sense CCHFV L, M, and S genome segments (strain IbAr10200; Genbank #KJ648913.1, #KJ648915.1, and #KJ648914.1, respectively) were transfected into Huh7 cells in conjunction with PolII-expression plasmids (pCAGGS) supplying CCHFV polymerase (RdRp), NP, and T7 polymerase in trans. The reporter CCHFV/ZsG was generated by substituting the full-length anti-genomic sense S segment for a modified version encoding ZsG. At 72 h post transfection, cell culture supernatants were harvested, clarified by low-speed centrifugation, and used to infect BSR-T7/5 cells. Virus stocks harvested 48 h post infection (hpi) from BSR-T7/5 cells were quantified by tissue culture infective dose 50 ($TCID_{50}$) assays in either SW13 (cytopathic effect) or BSR-T7/5 cells (immunofluorescence) (Reed and Muench, 1938).

2.3. Western blot analysis

Cell monolayers were harvested in 2 × Laemmli buffer (Bio-Rad), denatured at 95°C for 10 min, separated by SDS-PAGE using 4–12% bis-tris gels (Invitrogen), and transferred via semi-dry blotting to nitrocellulose membranes. Primary antibodies used were: α-CCHFV NP (IBT Bioservices, #04-0011), α-ZsGreen1 (Clonetech, #632598), and anti-α-tubulin (Sigma-Aldrich, #T5168). After probing with HRP-linked secondary antibodies (both Thermo-Fisher Scientific, #32260 and #32230), proteins were visualized using Fast Western Blot kit with SuperSignal West Dura HRP substrate (Thermo-Fisher), and protein bands imaged with the ChemiDoc MP system (Bio-Rad).

2.4. Passaging of CCHFV/ZsG

Huh7 cells (1×10^6 cells per T25 cell culture flask in 10 ml DMEM) were infected with CCHFV/ZsG at MOI 0.1. At either 48 or 72 hpi cell culture supernatant was removed, clarified by low-speed centrifugation, and 20 μl then used to infect a fresh T25 flask of Huh7 cells. This process was repeated for 10 virus passages. Prior to each passage the cell monolayer was monitored for ZsG expression, and at each passage viral RNA was extracted from the clarified supernatant for sequence analysis. Sequences were determined using the MiniSeq system (Illumina) and assembled using CLC Genomics Workbench 9 (Qiagen).

2.5. Antiviral compound screening

All compounds were obtained from either Selleckchem or Sigma-Aldrich with the exception of T-705 (BOC Sciences). Cells were seeded at either 1×10^4 cells/well (96-well plate) or 4×10^3 cells/well (384-well plate) 16–20 h prior to treatment with DMSO-diluted compounds (final DMSO concentration 0.5%). For the 384-well assay, compounds were added to the plate using an Echo acoustic liquid handler (Labcyte). Cells were infected 1 h post treatment, and at 72 hpi, either supernatants were collected or ZsG fluorescence was determined using a BioTek Synergy reader (height 6 mm; 100 gain/sensitivity). Cell viability (ATP content) was determined in parallel on compound-treated, mock-infected cells using CellTiter-Glo 2.0 (Promega). All experiments were performed in quadruplicate and repeated at least 3 times.

2.6. Microscopy and high-content imaging

ZsG fluorescence in infected cells was imaged directly using an EVOS digital inverted microscope (Thermo-Fisher). For immunofluorescence, cells were fixed in 10% formalin for 30 min, permeabilized in PBS containing 0.1% Triton-X100 (v/v) for 10 min, and blocked with PBS 5% BSA (v/v) for 30 min. Primary antibodies were either α-CCHFV NP (IBT Bioservices #04-0011) or α-CCHFV polyclonal hyper-immune mouse ascetic fluid (HMAF, in house), and secondary antibodies were labeled with AlexaFluor 555 (Thermo-Fisher, #A11034). Slides were mounted in DAPI-containing mounting media (Vector Shield). Microscopy images were taken using a Zeiss Axiovert 200 microscope using the 40 × objective. For high-content imaging, SW13 cells were seeded at 5×10^3 cells/well (96-well plate) 16–20 h prior to treatment. Cells were infected 2 h post treatment with CCHFV at MOI 0.1, and at 48 hpi cells were fixed, permeabilized, and stained with HMAF antibody, Nuc-Blue, and CellMask Red (Thermo-Fisher). Images were collected on the Operetta high-content imaging system (Perkin Elmer, US) using a 20 × objective and 9 fields per well, and data were analyzed using the Harmony software package (Perkin Elmer).

2.7. Data analysis

ZsG fluorescence values for compound-treated infected cells were normalized to mock-treated (DMSO only) cells, and used to fit a 4-parameter equation to semilog plots of the concentration-response data. From this, the compound concentrations inhibiting 50% of the ZsG expression (EC_{50}) were interpolated. Cell viability was similarly calculated in compound-treated mock-infected cells to determine the 50% cell cytotoxicity concentration (CC_{50}) of each compound. The selectivity index was calculated by dividing the CC_{50} by the EC_{50}. Data analysis was performed using GraphPad Prism v7. Suitability for high-throughput screening was determined using the Z prime (Z′) score, a measure of statistical effect size, with values between 0.5 and 1.0 considered acceptable (Zhang et al., 1999). The Bliss synergy analysis was performed using Combenefit software (http://www.cruk.cam.ac.uk/research-groups/jodrell-group/combenefit) (Di Veroli et al., 2016). Dose-response curves for each individual compound were combined to generate a dose-response surface for the reference (Bliss) model, from which the experimental surface and modelled surface were then compared. At each combination, deviations in the experimental surface from the modelled surface were attributed a percentage score indicating the degree of either synergy (increased effect) or antagonism (decreased effect). Significance was calculated using a one-sample *t*-test.

3. Results

3.1. Generation of a recombinant CCHFV expressing ZsGreen1

To generate a recombinant CCHFV expressing a fluorescent reporter protein, we constructed a modified S genome segment in which the ZsG coding sequence was inserted upstream of the NP coding sequence (Fig. 1a). The porcine teshovirus-1 2A peptide linker sequence (P2A) was included between ZsG and NP, allowing separate expression of both proteins via a ribosomal skipping event during P2A translation (Kim et al., 2011). ZsG was chosen as the reporter as it had previously generated strong fluorescence levels in analogous recombinant viral reporter assays, resulting in high signal-to-noise ratios and robust Z′ values (Albariño

et al., 2015; Welch et al., 2016). Furthermore, successful rescue of the recombinant CCHFV demonstrated that both ZsG and NP were able to tolerate the extra amino acid residues remaining at their C- and N- termini respectively after cleavage of P2A and remain functional.

The modified S segment was incorporated into the recently published CCHFV reverse genetics rescue system (Bergeron et al., 2015), allowing recovery of a CCHFV mutant (CCHFV/ZsG) producing green fluorescence in infected cells. Western blot analysis in CCHFV/ZsG infected Huh7 cells demonstrated efficient separation of NP and ZsG, although NP levels were lower than those in CCHFV-infected cells (Fig. 1b). ZsG distribution in CCHFV/ZsG infected cells was distinct from the NP, with the former evident in both cytoplasmic and nuclear compartments compared to the predominantly cytoplasmic NP (Fig. 1c). No CCHFV/ZsG infected cells were observed expressing NP but not ZsG, suggesting that the ZsG gene was stably incorporated into the CCHFV genome segment. Therefore, the P2A strategy adopted here appears extremely efficient at separating these 2 proteins, albeit resulting in reduced NP expression. Indeed, reduced expression of parental protein linked via P2A to a foreign protein has been described previously for other reporter viruses using this strategy (Albarino et al., 2015; Park et al., 2016; Reuther et al., 2015).

To establish the suitability of CCHFV/ZsG for studying CCHFV replication, we examined its growth kinetics in 3 human cell lines: Huh7, SW13, and HAP1. The human hepatocarcinoma Huh7 cell line was used because the liver is a major site of CCHFV replication, and this cell line has previously proved useful in the discovery and evaluation of antiviral compounds for other viral hemorrhagic fever pathogens such as Ebola, Marburg, and Lassa viruses (Mohr et al., 2015; Welch et al., 2016). The human adenocarcinoma SW13 cells are highly permissive to CCHFV and are a model cell line used to grow CCHFV stocks. In addition, we included a human haploid cell line (HAP1) that proved highly susceptible to CCHFV infection. These cell lines were infected with either CCHFV or CCHFV/ZsG at MOI 0.1, and titers ($TCID_{50}$/mL) were determined at 24, 48, and 72 hpi. In all cell lines tested, viral titers peaked at 48 hpi, with CCHFV/ZsG attenuated by approximately 0.5–1 logs in Huh7 and SW13 cells compared to CCHFV (Fig. 1d). The highest titers were observed in HAP1 cells, with CCHFV/ZsG attenuation also less pronounced. ZsG fluorescence increased throughout the time course, peaking at 72 hpi. The reduction in cytoplasmic NP levels is the likely cause of CCHFV/ZsG attenuation.

The genetic stability of CCHFV/ZsG was assessed by serially passaging the virus in Huh7 cells 10 times. Abundant ZsG fluorescence was evident in cell monolayers prior to each passage. Next generation sequence analysis of CCHFV/ZsG collected after 10 passages showed the modified S segment retained the ZsG-P2A-NP nucleotide sequence with no mutations observed. The only coding change observed throughout the 3 genome segments (threshold of > 5% of the reads in areas with > 1000 read coverage) was a 15% population in the M segment containing a I528L amino acid substitution caused by a single nucleotide change (Sup. Table 1). This suggests that the ZsG-P2A insertion is extremely stable and capable of sustaining viral replication over multiple passages.

3.2. Identification of CCHFV inhibitors using a screening assay

To optimize a screening assay incorporating CCHFV/ZsG, we assessed its activity in both Huh7 and SW13 cells treated with ribavirin, given this compound's established ability to inhibit CCHFV in vitro (Bergeron et al., 2010; Oestereich et al., 2016). Using 50 μM ribavirin as the positive control, and DMSO vehicle-only as the negative control, we optimized the assay for a 96-well plate format to give Z′ scores of 0.72 and 0.68, and signal-to-noise ratios of 50:1 and 45:1 for Huh7 and SW13 cells, respectively, indicating a robust assay. Dose-response curves with ribavirin demonstrated a concentration-dependent reduction in ZsG fluorescence in both cell lines, with EC_{50} values of 12.48 ± 2.61 and 5.69 ± 0.71 μM for Huh7 and SW13 cells, respectively (Fig. 2a). These values are similar to the previously reported EC_{50} of 11.5 μM in Vero-E6 cells (Oestereich et al., 2014), indicating that the virus was suitable for inclusion into a screening assay using reduction in ZsG fluorescence as an indicator of viral replication inhibition.

Using Huh7 cells, the optimized assay was used to screen a panel of 38 nucleoside analogs for their potential to inhibit CHFV replication. This panel was further supplemented with mycophenolic acid (MPA) and its pro-drug mycophenolate mofetil (MMF), which, like ribavirin, are both inosine-5′-monophosphate dehydrogenase (IMPDH) inhibitors. While the mechanism by which ribavirin inhibits CCHFV is still unknown, one proposal is that IMPDH inhibition by ribavirin reduces the intracellular GTP nucleotide pool available for RNA synthesis. Therefore, MPA and MMF, previously shown to have antiviral effects against viruses like influenza, dengue, Zika, rotavirus, and hantavirus (Barrows et al., 2016; Diamond et al., 2002; Sun et al., 2007; To et al., 2016; Yin et al., 2016), were included in the screen. Inhibition was initially assessed for each compound at 5000, 500, and 50 nM, with cell viability confirmed concurrently (Sup. Table 2). Of the 40 compounds tested, 4 – T-705, 2′-dFC, MPA, and MMF – demonstrated robust anti-CCHFV activity (ZsG fluorescence reduced to < 30% of control) with > 80% cell viability, and warranted further evaluation (Table 1).

Dose-response curves with these 4 compounds showed a concentration-dependent reduction in ZsG fluorescence (Fig. 2b). The T-705 EC_{50} value (1.03 ± 0.16 μM) was lower than the 7 μM previously reported (Oestereich et al., 2014), possibly due to different cell lines used. Both MPA (EC_{50} = 100 ± 10 nM) and MMF (EC_{50} = 390 ± 130 nM) demonstrated greater inhibition of CCHFV than either ribavirin or T-705, although cell viability was reduced at higher concentrations, resulting in reduced selectivity indices for both. Most promising were the results for 2′-dFC, which exhibited the greatest potency of all the compounds evaluated (EC_{50} = 61 ± 18 nM) with no cytotoxicity at the highest concentration tested. To confirm that the antiviral activity was not due to factors affecting reporter stability or expression, and therefore specific to CCHFV/ZsG, the compounds' ability to inhibit wild-type CCHFV replication was tested (Fig. 2c). CCHFV titers in cells treated with T-705, 2′-dFC, and ribavirin were reduced in a concentration-dependent manner, with no virus detected at the highest concentration of compound tested. Due to the similarity between MPA and MMF in inhibiting CCHFV, only MPA was tested in the titer reduction assay because of its superior SI. In MPA-treated cells, a dose-dependent viral titer reduction was observed, with an approximate 2.5 log reduction at the highest concentration, although this reduction was not

as pronounced as that induced by the other compounds. Therefore, while MPA and MMF both demonstrated potent sub-micromolar inhibition of CCHFV, their cytotoxicity at low micromolar concentrations and subsequently low SI values limit their potential as future CCHFV antivirals.

With 2′-dFC emerging as the most promising candidate from the screening assay, we further examined its inhibitory effect using a high-content imaging assay. SW13 cells treated with a range of 2′-dFC concentrations were infected with CCHFV at MOI 0.1, and viral protein production was examined 48 hpi. The percentage of infected cells at each concentration was calculated by counting the number of individual cells expressing CCHFV protein from the total number of cells counted, giving an EC_{50} of 95 nM (Fig. 3a). Cell viability was determined by nuclei count (Fig. 3b). The reduction in CCHFV protein expression was clearly evident with increasing concentrations of 2′-dFC (Fig. 3c). Therefore, 2′-dFC potently inhibited CCHFV replication, with sub-micromolar EC_{50} values determined via 2 independent assays, and with no associated cytotoxicity at the highest concentrations evaluated.

3.3. Synergy between 2′-dFC and T-705 in inhibiting CCHFV replication

Given both the standard use of ribavirin in CCHF treatment and the potential of T-705 as a future therapeutic option, we next investigated whether either of these drugs would synergize with 2′-dFC. A 6 × 6 concentration matrix was designed according to the EC_{50} values for each compound, with 3 drug combinations tested: T-705 with ribavirin; 2′-dFC with ribavirin; and 2′-dFC with T-705. Using the 384-well assay, Huh7 cells were infected with CCHFV/ZsG at MOI 0.1 and ZsG fluorescence was measured at 3 dpi. The T-705 vs. ribavirin combination exhibited synergistic activity according to the Bliss independence model, with a 53 ± 6% increase in fluorescence inhibition in cells treated with both 2 μM T-705 and 3.3 μM ribavirin compared to predicted levels (Fig. 4a). This is similar to the enhanced inhibition of CCHFV observed for this combination of compounds in Vero-E6 cells (Oestereich et al., 2014). The 2′-dFC vs. T-705 combination also demonstrated synergy, with a 51 ± 6% synergistic effect observed with a combination of 2 μM T-705 and 210 nM 2′-dFC (Fig. 4b). Synergy was not seen in any combination of 2′-dFC with ribavirin, with effects predominantly additive (Fig. 4c).

Confirmatory screening was performed using wild-type CCHFV for those combinations of T-705 with ribavirin, and 2′-dFC with T-705 again exhibited the strongest synergy (Fig. 5a). In Huh7 cells treated with 2 μM T-705 or 200 nM 2′-dFC alone, CCHFV titers were significantly ($p = 0.0001$) reduced by approximately 2 logs compared to a DMSO only-treated control. However, in cells treated with a combination of these compounds at the same concentrations, titers were further significantly ($p = 0.0001$) reduced to below the limit of detection of the assay (< 18.9 $TCID_{50}$/mL). A similar pattern was observed in cells treated with T-705 or ribavirin (10 μM) alone or in combination. While the effect of 2′-dFC vs. ribavirin was shown to be only additive, viral titers in cells treated with a combination of these drugs were also significantly ($p = 0.0001$) reduced compared to titers in cells treated with the compounds individually. A combination of all 3 compounds together also significantly reduced viral titers compared to DMSO-treated and individually-treated cells,

reducing viral titers to below the limit of detection of the assay. Cell viability was determined concurrently for all combinations evaluated and no cytotoxicity was observed (Fig. 5b). These data hold promise for a potential combination treatment for CCHF using 2′-dFC with either T-705 or ribavirin.

4. Discussion

Here we describe the development of a recombinant CCHFV expressing a fluorescent reporter protein which, although slightly attenuated compared to the wild-type virus, is a suitable surrogate for studying the CCHFV life cycle. Incorporation of the recombinant virus into a high-throughput screening assay allowed us to identify compounds with antiviral effects on the virus lifecycle. Previously, screening of potential CCHFV antivirals was limited to small-scale investigations due to the labor-intensive methods required to quantify CCHFV inhibition. These approaches are effective when considering compounds with known antiviral effects, such as the broad-spectrum antiviral ribavirin or the anti-influenza compound T-705, but investigations of large compound libraries are challenging because these assays are not readily adaptable to high-throughput screening processes. However, generating a reporter CCHFV, for which post-infection processing time is reduced to simply quantifying ZsG fluorescence, will allow us to more rapidly investigate a broader range of potential antiviral compounds.

The observation that 2′-dFC is a potent inhibitor of CCHFV is in line with data showing that it also inhibits several other viruses, such as hepatitis C virus (HCV), influenza virus, and Lassa virus (Kumaki et al., 2011; Stuyver et al., 2004; Welch et al., 2016). Derivatives of 2′-dFC have shown promise as anti-HCV compounds, with several progressing to clinical trials (Pierra et al., 2006; Pockros et al., 2013; Wedemeyer et al., 2013). However, concerns remain over the long-term adverse effects of treatment with 2′-deoxynucleoside analogs, which are predominately precipitated by mitochondrial toxicity (Arnold et al., 2012). However, unlike HCV, CCHFV is an acute infection that would not require prolonged treatment, reducing the potential for toxicity observed with long-term 2′-deoxynucleoside analog treatment regimens (Lee et al., 2003). Indeed, *in vivo* toxicology studies with 2′-dFC using rats and woodchucks showed no adverse clinical effects after 90-day treatments (Richardson et al., 1999). Further experiments to investigate toxicity and confirm the *in vivo* anti-CCHFV effects of 2′-dFC are planned using available animal models of disease (Bente et al., 2010; Spengler et al., 2017; Zivcec et al., 2013).

In addition to antiviral discovery, CCHFV/ZsG has other key applications, including facilitating studies of viral pathogenesis. In HAP1 cells, CCHFV/ZsG grows to higher titers and exhibits a less attenuated phenotype than in the other cell types tested here. Additional investigations of CCHFV/ZsG in HAP1 cells using gene-trapping methods offers extensive opportunities to study host-pathogen interactions at the cellular level. A HAP1 screening assay was recently used to identify viral entry co-factors for both Ebola and Lassa viruses (Carette et al., 2011; Jae et al., 2013). Events determining the progression of CCHFV infection are still unclear, including what cells are initially targeted by the virus, and where virus is distributed in the infected host. Combining CCHFV/ZsG with techniques such as

FACS analysis to identify cell tropism, or with *in vivo* imaging to determine the progression of viral dissemination throughout disease will allow us to better investigate these processes.

In conclusion, we have developed a reporter CCHFV and optimized its use in a rapid and efficient antiviral screening assay. In addition to confirming the previously reported antiviral effects of both ribavirin and T-705, we identified and quantified the potent antiviral effects of 2′-dFC on CCHFV replication, and demonstrated its potential for a combination therapy with T-705. As well as being useful in identifying compounds capable of inhibiting viral replication, CCHFV/ZsG can also greatly facilitate the study of the CCHFV life cycle using fluorescent-based detection assays. Such studies will aid in our understanding of CCHFV, an important emerging human pathogen.

Supplementary Material

Refer to Web version on PubMed Central for supplementary material.

Acknowledgements

We thank Tatyana Klimova for assistance with editing this manuscript. The findings and conclusions in this report are those of the authors and do not necessarily represent the official position of the CDC. Stephen Welch holds a fellowship supported by the Research Participation Program at the CDC administered by the Oak Ridge Institute for Science and Education through an interagency agreement between the U.S. Department of Energy (DOE) and CDC.

References

Albarino CG, Wiggleton Guerrero L, Lo MK, Nichol ST, Towner JS, 2015. Development of a reverse genetics system to generate a recombinant Ebola virus Makona expressing a green fluorescent protein. Virology 484, 259–264. 10.1016/j.virol.2015.06.013. [PubMed: 26122472]

Albariño CG, Wiggleton Guerrero L, Lo MK, Nichol ST, Towner JS, 2015. Development of a reverse genetics system to generate a recombinant Ebola virus Makona expressing a green fluorescent protein. Virology 484, 259–264. 10.1016/j.virol.2015.06.013. [PubMed: 26122472]

Arnold JJ, Sharma SD, Feng JY, Ray AS, Smidansky ED, Kireeva ML, Cho A, Perry J, Vela JE, Park Y, Xu Y, Tian Y, Babusis D, Barauskus O, Peterson BR, Gnatt A, Kashlev M, Zhong W, Cameron CE, 2012. Sensitivity of mitochondrial transcription and resistance of RNA polymerase II dependent nuclear transcription to antiviral ribonucleosides. PLoS Pathog. 8, e1003030. 10.1371/journal.ppat.1003030. [PubMed: 23166498]

Ascioglu S, Leblebicioglu H, Vahaboglu H, Chan KA, 2011. Ribavirin for patients with Crimean-Congo haemorrhagic fever: a systematic review and meta-analysis. J. Antimicrob. Chemother 66, 1215–1222. 10.1093/jac/dkr136. [PubMed: 21482564]

Barrows NJ, Campos RK, Powell ST, Prasanth KR, Schott-Lerner G, Soto-Acosta R, Galarza-Muñoz G, McGrath EL, Urrabaz-Garza R, Gao J, Wu P, Menon R, Saade G, Fernandez-Salas I, Rossi SL, Vasilakis N, Routh A, Bradrick SS, Garcia-Blanco MA, 2016. A screen of FDA-approved drugs for inhibitors of Zika virus infection. Cell Host Microbe 20, 259–270. 10.1016/j.chom.2016.07.004. [PubMed: 27476412]

Bente DA, Alimonti JB, Shieh W-J, Camus G, Ströher U, Zaki S, Jones SM, 2010. Pathogenesis and immune response of Crimean-Congo hemorrhagic fever virus in a STAT-1 knockout mouse model. J. Virol 84, 11089–11100. 10.1128/JVI.01383-10. [PubMed: 20739514]

Bente DA, Forrester NL, Watts DM, McAuley AJ, Whitehouse CA, Bray M, 2013. Crimean-Congo hemorrhagic fever: history, epidemiology, pathogenesis, clinical syndrome and genetic diversity. Antivir. Res 100, 159–189. 10.1016/j.antiviral.2013.07.006. [PubMed: 23906741]

Bergeron É, Albariño CG, Khristova ML, Nichol ST, 2010. Crimean-Congo hemorrhagic fever virus-encoded ovarian tumor protease activity is dispensable for virus RNA polymerase function. J. Virol 84, 216–226. 10.1128/JVI.01859-09. [PubMed: 19864393]

Bergeron É, Zivcec M, Chakrabarti AK, Nichol ST, Albariño CG, Spiropoulou CF, 2015. Recovery of recombinant crimean Congo hemorrhagic fever virus reveals a function for non-structural glycoproteins cleavage by furin. PLoS Pathog. 11, e1004879. 10.1371/journal.ppat.1004879. [PubMed: 25933376]

Carette JE, Raaben M, Wong AC, Herbert AS, Obernosterer G, Mulherkar N, Kuehne AI, Kranzusch PJ, Griffin AM, Ruthel G, Dal Cin P, Dye JM, Whelan SP, Chandran K, Brummelkamp TR, 2011. Ebola virus entry requires the cholesterol transporter Niemann-Pick C1. Nature 477, 340–343. 10.1038/nature10348. [PubMed: 21866103]

Di Veroli GY, Fornari C, Wang D, Mollard S, Bramhall JL, Richards FM, Jodrell DI, 2016. Combenefit: an interactive platform for the analysis and visualization of drug combinations. Bioinformatics 32, 2866–2868. 10.1093/bioinformatics/btw230. [PubMed: 27153664]

Diamond MS, Zachariah M, Harris E, 2002. Mycophenolic acid inhibits dengue virus infection by preventing replication of viral RNA. Virology 304, 211–221. [PubMed: 12504563]

Dokuzoguz B, Celikbas AK, Gök ŞE, Baykam N, Eroglu MN, Ergönül O, 2013. Severity scoring index for Crimean-Congo hemorrhagic fever and the impact of ribavirin and corticosteroids on fatality. Clin. Infect. Dis 57, 1270–1274. 10.1093/cid/cit527. [PubMed: 23946218]

Hoogstraal H, 1979. The epidemiology of tick-borne Crimean-Congo hemorrhagic fever in Asia, Europe, and Africa. J. Med. Entomol 15, 307–417. [PubMed: 113533]

Humolli I, Dedushaj I, Zupanac TA, Muçaj S, 2010. Epidemiological, serological and herd immunity of Crimean-Congo haemorrhagic fever in Kosovo. Med. Arh 64, 91–93. [PubMed: 20514773]

Jae LT, Raaben M, Riemersma M, van Beusekom E, Blomen VA, Velds A, Kerkhoven RM, Carette JE, Topaloglu H, Meinecke P, Wessels MW, Lefeber DJ, Whelan SP, van Bokhoven H, Brummelkamp TR, 2013. Deciphering the glycosylome of dystroglycanopathies using haploid screens for lassa virus entry. Science 340, 479–483. 10.1126/science.1233675. [PubMed: 23519211]

Kim JH, Lee S-R, Li L-H, Park H-J, Park J-H, Lee KY, Kim M-K, Shin BA, Choi S-Y, 2011. High cleavage efficiency of a 2A peptide derived from porcine teschovirus-1 in human cell lines, zebrafish and mice. PLoS One 6, e18556. 10.1371/journal.pone.0018556. [PubMed: 21602908]

Köksal I, Yilmaz G, Aksoy F, Aydin H, Yavuz I, Iskender S, Akcay K, Erensoy S, Caylan R, Aydin K, 2010. The efficacy of ribavirin in the treatment of Crimean-Congo hemorrhagic fever in Eastern Black Sea region in Turkey. J. Clin. Virol 47, 65–68. 10.1016/j.jcv.2009.11.007. [PubMed: 19962342]

Kuhn JH, Wiley MR, Rodriguez SE, Bào Y, Prieto K, Travassos da Rosa APA, Guzman H, Savji N, Ladner JT, Tesh RB, Wada J, Jahrling PB, Bente DA, Palacios G, 2016. Genomic characterization of the genus nairovirus (family bunyaviridae). Viruses 8, 164. 10.3390/v8060164.

Kumaki Y, Day CW, Smee DF, Morrey JD, Barnard DL, 2011. In vitro and in vivo efficacy of fluorodeoxycytidine analogs against highly pathogenic avian influenza H5N1, seasonal, and pandemic H1N1 virus infections. Antivir. Res 92, 329–340. 10.1016/j.antiviral.2011.09.001. [PubMed: 21925541]

Leblebicioglu H, Ozaras R, Irmak H, Sencan I, 2016. Crimean-Congo hemorrhagic fever in Turkey: current status and future challenges. Antivir. Res 126, 21–34. 10.1016/j.antiviral.2015.12.003. [PubMed: 26695860]

Lee H, Hanes J, Johnson KA, 2003. Toxicity of nucleoside analogues used to treat AIDS and the selectivity of the mitochondrial DNA polymerase. Biochemistry 42, 14711–14719. 10.1021/bi035596s. [PubMed: 14674745]

Mishra AC, Mehta M, Mourya DT, Gandhi S, 2011. Crimean-Congo haemorrhagic fever in India. Lancet 378, 372. 10.1016/S0140-6736(11)60680-6. [PubMed: 21784269]

Mohr EL, McMullan LK, Lo MK, Spengler JR, Bergeron É, Albariño CG, Shrivastava-Ranjan P, Chiang C-F, Nichol ST, Spiropoulou CF, Flint M, 2015. Inhibitors of cellular kinases with broad-spectrum antiviral activity for hemorrhagic fever viruses. Antivir. Res 120, 40–47. 10.1016/j.antiviral.2015.05.003. [PubMed: 25986249]

Oestereich L, Rieger T, Ludtke A, Ruibal P, Wurr S, Pallasch E, Bockholt S, Krasemann S, Munoz-Fontela C, Gunther S, 2016. Efficacy of favipiravir alone and in combination with ribavirin in a lethal, immunocompetent mouse model of lassa fever. J. Infect. Dis 213, 934–938. 10.1093/infdis/jiv522. [PubMed: 26531247]

Oestereich L, Rieger T, Neumann M, Bernreuther C, Lehmann M, Krasemann S, Wurr S, Emmerich P, de Lamballerie X, Ölschläger S, Günther S, 2014. Evaluation of antiviral efficacy of ribavirin, arbidol, and T-705 (favipiravir) in a mouse model for Crimean-Congo hemorrhagic fever. PLoS Negl. Trop. Dis 8, e2804. 10.1371/journal.pntd.0002804. [PubMed: 24786461]

Ozbey SB, Kader Ç, Erbay A, Ergönül O, 2014. Early use of ribavirin is beneficial in Crimean-Congo hemorrhagic fever. Vector Borne Zoonotic Dis. 14, 300–302. 10.1089/vbz.2013.1421. [PubMed: 24689859]

Park A, Yun T, Hill TE, Ikegami T, Juelich TL, Smith JK, Zhang L, Freiberg AN, Lee B, 2016. Optimized P2A for reporter gene insertion into Nipah virus results in efficient ribosomal skipping and wild-type lethality. J. Gen. Virol 97, 839–843. 10.1099/jgv.0.000405. [PubMed: 26781134]

Pierra C, Amador A, Benzaria S, Cretton-Scott E, D'Amours M, Mao J, Mathieu S, Moussa A, Bridges EG, Standring DN, Sommadossi J-P, Storer R, Gosselin G, 2006. Synthesis and pharmacokinetics of valopicitabine (NM283), an efficient pro-drug of the potent anti-HCV agent 2'-C-methylcytidine. J. Med. Chem 49, 6614–6620. 10.1021/jm0603623. [PubMed: 17064080]

Pockros PJ, Jensen D, Tsai N, Taylor R, Ramji A, Cooper C, Dickson R, Tice A, Kulkarni R, Vierling JM, Lou Munson M, Chen Y-C, Najera I, Thommes J, JUMP-C Investigators, 2013. JUMP-C: a randomized trial of mericitabine plus pegylated interferon alpha-2a/ribavirin for 24 weeks in treatment-naïve HCV genotype 1/4 patients. Hepatology 58, 514–523. 10.1002/hep.26275. [PubMed: 23359491]

Reed LJ, Muench H, 1938. A simple method of estimating fifty per cent endpoints. 27, 493–497.

Reuther P, Göpfert K, Dudek AH, Heiner M, Herold S, Schwemmle M, 2015. Generation of a variety of stable Influenza A reporter viruses by genetic engineering of the NS gene segment. Sci. Rep 5, 11346. 10.1038/srep11346. [PubMed: 26068081]

Richardson FC, Tennant BC, Meyer DJ, Richardson KA, Mann PC, McGinty GR, Wolf JL, Zack PM, Bendele RA, 1999. An evaluation of the toxicities of 2"-fluorouridine and 2-"fluorocytidine-HCl in F344 rats and woodchucks (Marmota monax). Toxicol. Pathol 27, 607–617. 10.1177/019262339902700601. [PubMed: 10588540]

Soares-Weiser K, Thomas S, Thomson G, Garner P, 2010. Ribavirin for Crimean-Congo hemorrhagic fever: systematic review and meta-analysis. BMC Infect. Dis 10, 207. 10.1186/1471-2334-10-207. [PubMed: 20626907]

Spengler JR, Keating MK, McElroy AK, Zivcec M, Coleman-McCray JD, Harmon JR, Bollweg BC, Goldsmith CS, Bergeron É, Keck JG, Zaki SR, Nichol ST, Spiropoulou CF, 2017. Crimean-Congo hemorrhagic fever in humanized mice reveals glial cells as primary targets of neurological infection. J. Infect. Dis 10.1093/infdis/jix215.

Stuyver LJ, McBrayer TR, Whitaker T, Tharnish PM, Ramesh M, Lostia S, Cartee L, Shi J, Hobbs A, Schinazi RF, Watanabe KA, Otto MJ, 2004. Inhibition of the subgenomic hepatitis C virus replicon in huh-7 cells by 2"-deoxy-2-"fluorocytidine. Antimicrob. Agents Chemother 48, 651–654. 10.1128/AAC.48.2.651-654.2004. [PubMed: 14742230]

Sun Y, Chung D-H, Chu Y-K, Jonsson CB, Parker WB, 2007. Activity of ribavirin against Hantaan virus correlates with production of ribavirin-5'-triphosphate, not with inhibition of IMP dehydrogenase. Antimicrob. Agents Chemother 51, 84–88. 10.1128/AAC.00790-06. [PubMed: 17060520]

Tasdelen Fisgin N, Ergonul O, Doganci L, Tulek N, 2009. The role of ribavirin in the therapy of Crimean-Congo hemorrhagic fever: early use is promising. Eur. J. Clin. Microbiol. Infect. Dis 28, 929–933. 10.1007/s10096-009-0728-2.

To KKW, Mok K-Y, Chan ASF, Cheung NN, Wang P, Lui Y-M, Chan JFW, Chen H, Chan K-H, Kao RYT, Yuen K-Y, 2016. Mycophenolic acid, an immunomodulator, has potent and broad-spectrum in vitro antiviral activity against pandemic, seasonal and avian influenza viruses affecting humans. J. Gen. Virol 97, 1807–1817. 10.1099/jgv.0.000512. [PubMed: 27259985]

Wedemeyer H, Jensen D, Herring R, Ferenci P, Ma M-M, Zeuzem S, Rodriguez-Torres M, Bzowej N, Pockros P, Vierling J, Ipe D, Munson ML, Chen Y-C, Najera I, Thommes J, Investigators PROPEL, 2013. PROPEL: a randomized trial of mericitabine plus peginterferon alpha-2a/ribavirin therapy in treatment-naïve HCV genotype 1/4 patients. Hepatology 58, 524–537. 10.1002/hep.26274. [PubMed: 23348636]

Welch SR, Guerrero LW, Chakrabarti AK, McMullan LK, Flint M, Bluemling GR, Painter GR, Nichol ST, Spiropoulou CF, Albariño CG, 2016. Lassa and Ebola virus inhibitors identified using minigenome and recombinant virus reporter systems. Antivir. Res 136, 9–18. 10.1016/j.antiviral.2016.10.007. [PubMed: 27771389]

WHO, 2016. Blueprint for R & D Preparedness and Response to Public Health Emergencies Due to Highly Infectious Pathogens.

Yin Y, Wang Y, Dang W, Xu L, Su J, Zhou X, Wang W, Felczak K, van der Laan LJW, Pankiewicz KW, van der Eijk AA, Bijvelds M, Sprengers D, de Jonge H, Koopmans MPG, Metselaar HJ, Peppelenbosch MP, Pan Q, 2016. Mycophenolic acid potently inhibits rotavirus infection with a high barrier to resistance development. Antivir. Res 133, 41–49. 10.1016/j.antiviral.2016.07.017. [PubMed: 27468950]

Zhang JH, Chung TD, Oldenburg KR, 1999. A simple statistical parameter for use in evaluation and validation of high throughput screening assays. J. Biomol. Screen 4, 67–73. [PubMed: 10838414]

Zivcec M, Safronetz D, Scott D, Robertson S, Ebihara H, Feldmann H, 2013. Lethal Crimean-Congo hemorrhagic fever virus infection in interferon α/β receptor knockout mice is associated with high viral loads, proinflammatory responses, and coagulopathy. J. Infect. Dis 207, 1909–1921. 10.1093/infdis/jit061. [PubMed: 23417661]

Zivcec M, Scholte F, Spiropoulou C, Spengler J, Bergeron É, 2016. Molecular insights into Crimean-Congo hemorrhagic fever virus. Viruses 8, 106. 10.3390/v8040106. [PubMed: 27110812]

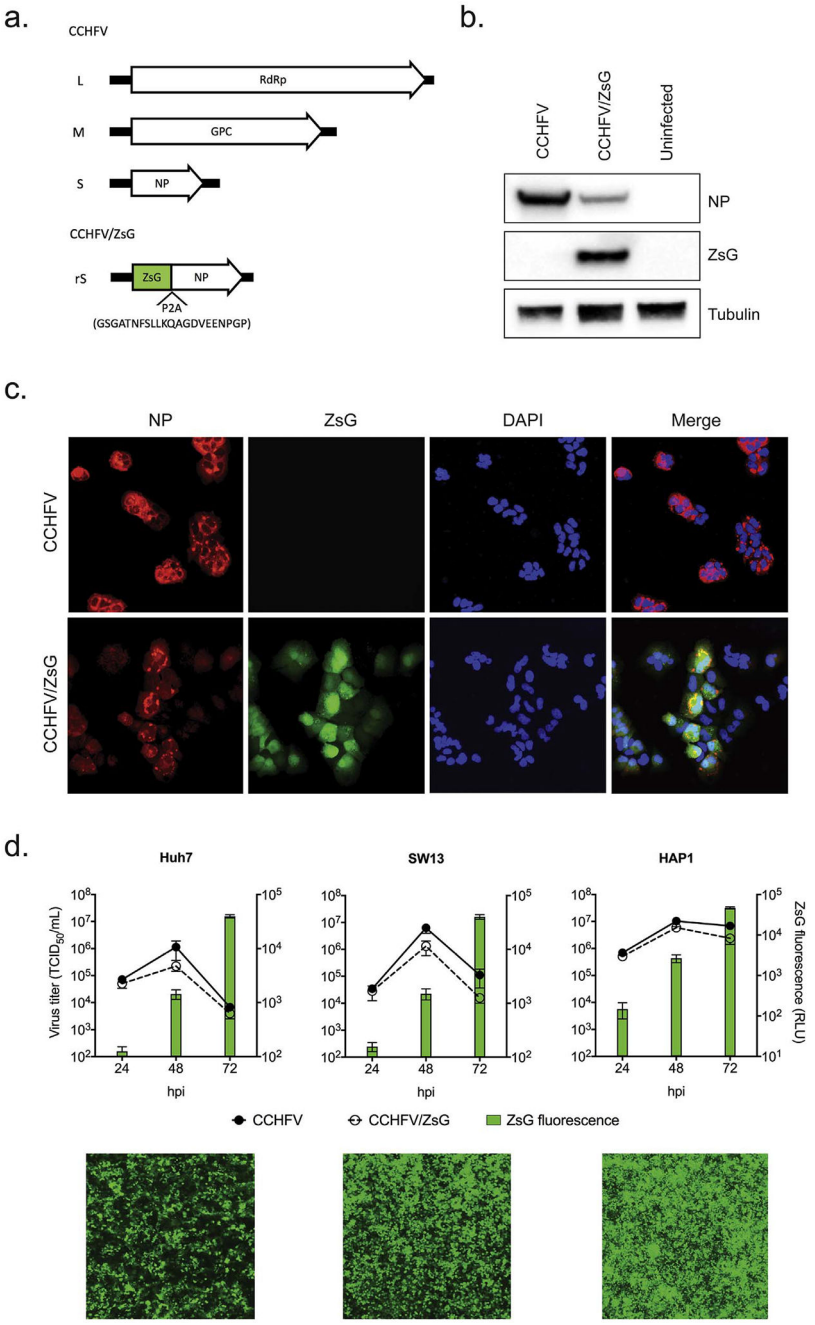

Fig. 1. Design and characterization of CCHFV/ZsG.

a. Schematic representation of the large (L), medium (M), and small (S) genome segments (antigenomic sense) of Crimean-Congo hemorrhagic fever virus (CCHFV). Arrows represent the viral protein coding sequences for RNA-dependent RNA polymerase (RdRp), glycoprotein precursor (GPC), and nucleoprotein (NP). CCHFV strain IbAr10200 S segment was modified by inserting the ZsGreen1 (ZsG) protein coding sequence fused to the P2A sequence (amino acid sequence shown) upstream of the NP coding region (rS). **b.** Western blot analysis of viral protein expression in Huh7 cells infected with CCHFV/ZsG at MOI 1. Cell lysates were harvested 72 h post infection (hpi) to determine cellular expression levels

of NP and ZsG, using tubulin as a loading control. **c.** Cellular localization of virally expressed proteins. Huh7 cells were infected with either CCHFV or CCHFV/ZsG at MOI 1, and imaged 48 hpi. CCHFV NP was detected using immunofluorescence, and ZsG fluorescence was imaged using standard fluorescent microscopy. **d.** Viral growth curves in Huh7, SW13, and HAP1 cells infected with either CCHFV or CCHFV/ZsG at MOI 0.1. Titers ($TCID_{50}$) were determined at 24, 48, and 72 hpi, with ZsG fluorescence determined concurrently at the same time points (RLU, relative light units). Representative fluorescent microscopy images of CCHFV/ZsG-infected cell monolayers at 72 hpi are presented.

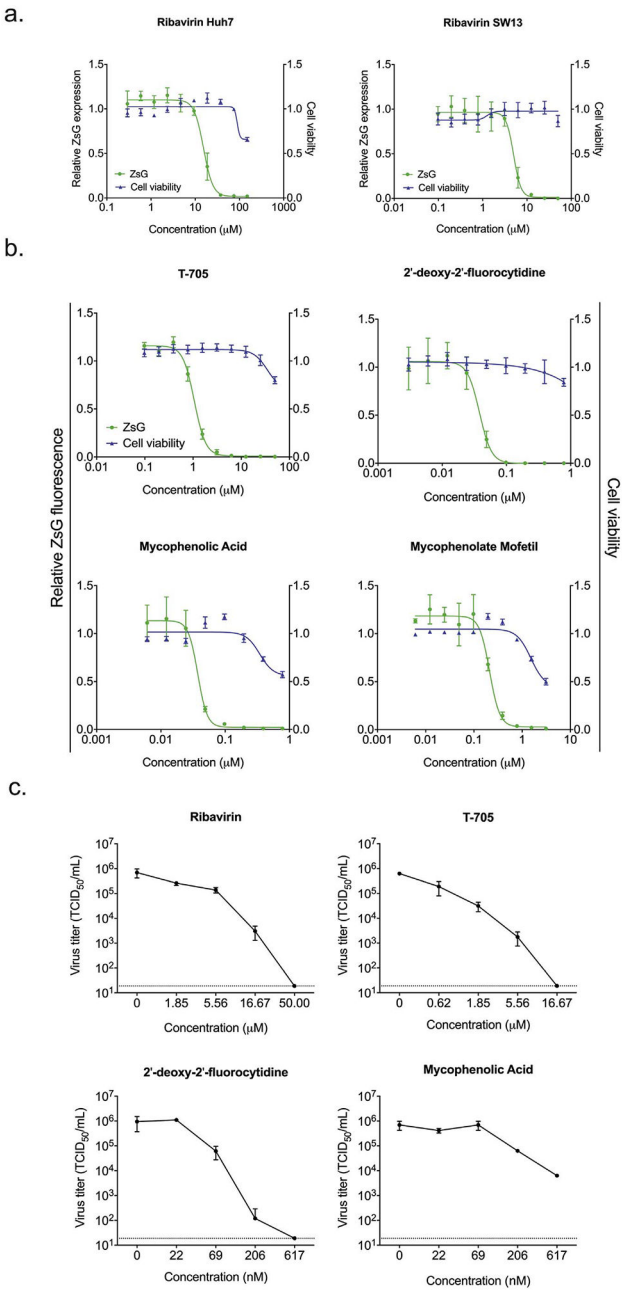

Fig. 2. Antiviral activity of compounds selected by the screening assay.

a. Dose-response curves in Huh7 or SW13 cells treated with a 2-fold serial dilution of ribavirin before infection with CCHFV/ZsG at MOI 0.1. At 72 h post treatment, the reduction in ZsG fluorescence (green) was determined, and all values were normalized to those in mock-treated (DMSO only) cells. Cell viability was determined concurrently using the same serial-fold dilution of compound, with ATP content (blue) normalized to content in mock-treated cells. Each point represents the mean of quadruplicate wells, with error bars indicating standard deviation. Graphs are representative of 3 independent experiments. **b.** Representative concentration-response curves in Huh7 cells infected with CCHFV/ZsG and treated with T-705, 2′-deoxy-2′-fluorocytidine (2′-dFC), mycophenolic acid, or

mycophenolate mofetil. Each point represents the mean of quadruplicate wells, with error bars indicating standard deviation. Graphs are representative of 3 independent experiments. **c.** Confirmatory counter-screen titer reduction assays were performed using wild-type CCHFV. Huh7 cells were treated with 4 dilutions of each compound centered around their calculated EC_{50} value 1 h prior to infection with CCHFV at MOI 0.1. At 48 hpi, virus-containing supernatants were harvested, and viral titers were determined by $TCID_{50}$. Each point represents the mean of triplicate wells, with error bars indicating standard deviation. Dotted line represents the limit of detection for this assay (1.89×10^1 $TCID_{50}$/mL). (For interpretation of the references to colour in this figure legend, the reader is referred to the web version of this article.)

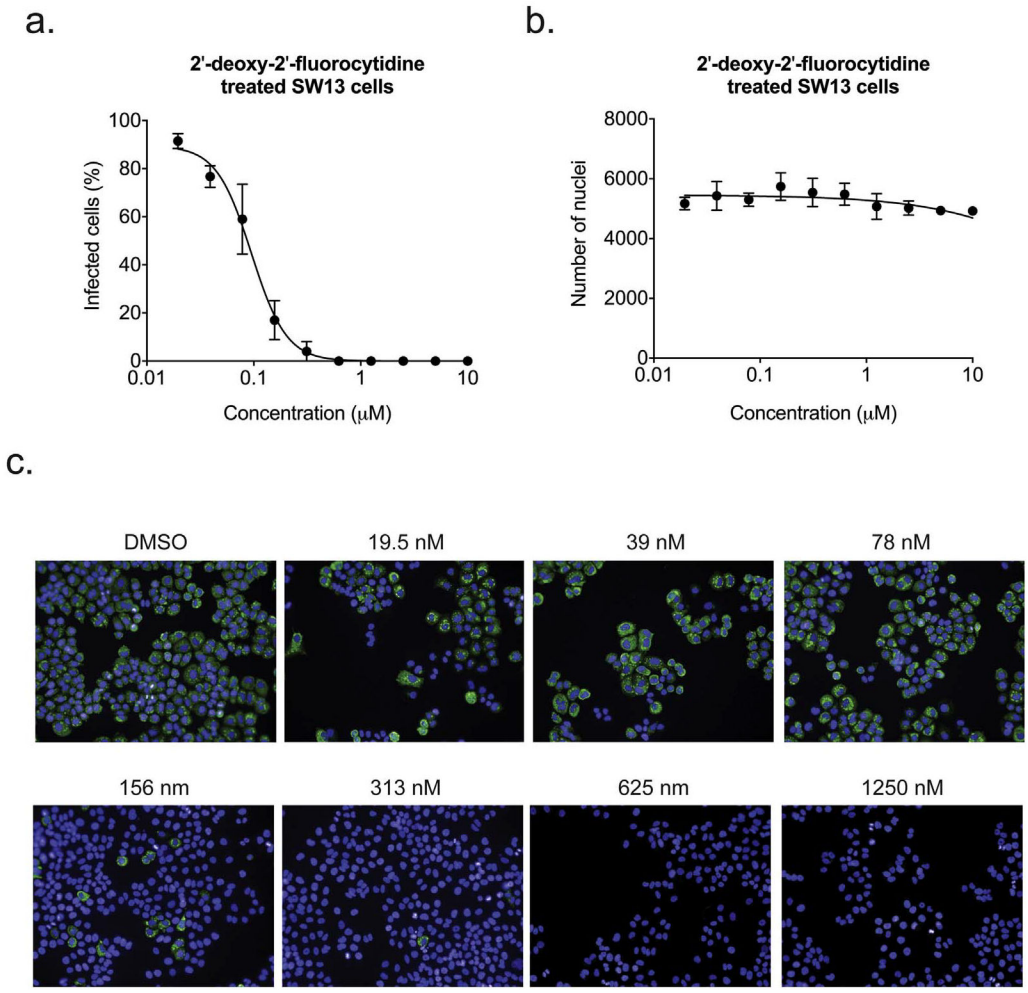

Fig. 3. 2′-dFC inhibition of CCHFV visualized using high-content imaging.

Dose-response curve in SW13 cells treated with a 2-fold serial dilution of 2′-dFC before infection with CCHFV at MOI 0.1. At 48 hpi, cells were fixed and stained with anti-CCHFV polyclonal antibodies, CellMask Red, and Nuc-Blue to visualize viral proteins, cell cytoplasm, and cell nuclei, respectively. **a.** The percentage of infected cells at each concentration of compound was calculated by determining the proportion of cells expressing CCHFV proteins compared to total cell number (based on CellMask Red). **b.** Cell viability assessed by determining the number of Nuc-Blue-stained nuclei. **c.** Representative images at indicated 2′-dFC concentrations show the reduction in CCHFV protein production (green) in the absence of any cytotoxicity (Nuc-Blue-stained nuclei). CellMask Red staining was omitted from these images for clarity. (For interpretation of the references to colour in this figure legend, the reader is referred to the web version of this article.)

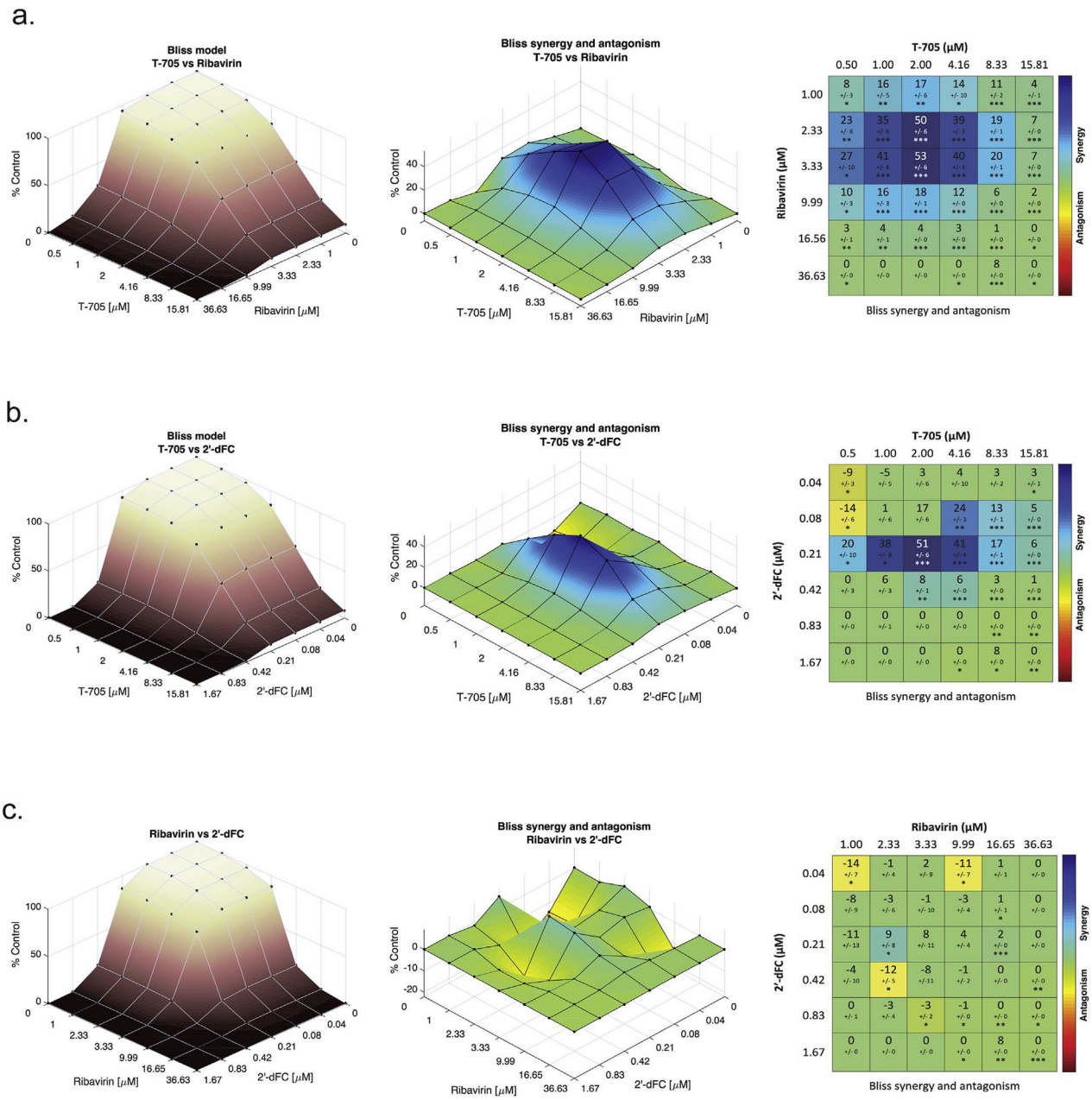

Fig. 4. Synergistic effects of 2′-dFC with ribavirin or T-705.

Huh7 cells were treated with a 6 × 6 compound combination matrix prior to infection with CCHFV/ZsG at MOI 0.1. At 72 h post treatment, the reduction in ZsG fluorescence was determined, and all values normalized to mock-treated (DMSO only) cells. The compound combinations evaluated were: **a.** T-705 with ribavirin; **b.** T-705 with 2′-dFC; and **c.** 2′-dFC with ribavirin. Dose-response surface curves were created for each combination (Bliss model), from which Bliss synergy and antagonism surface isograms were generated. Matrix tables indicate the maximum synergy value for each combination (% synergy effect observed over expected), with standard deviation indicated. Significance of synergy effect

over expected results is indicated following a one-sample *t*-test (*p < 0.05; **p < 0.01, ***p < 0.001).

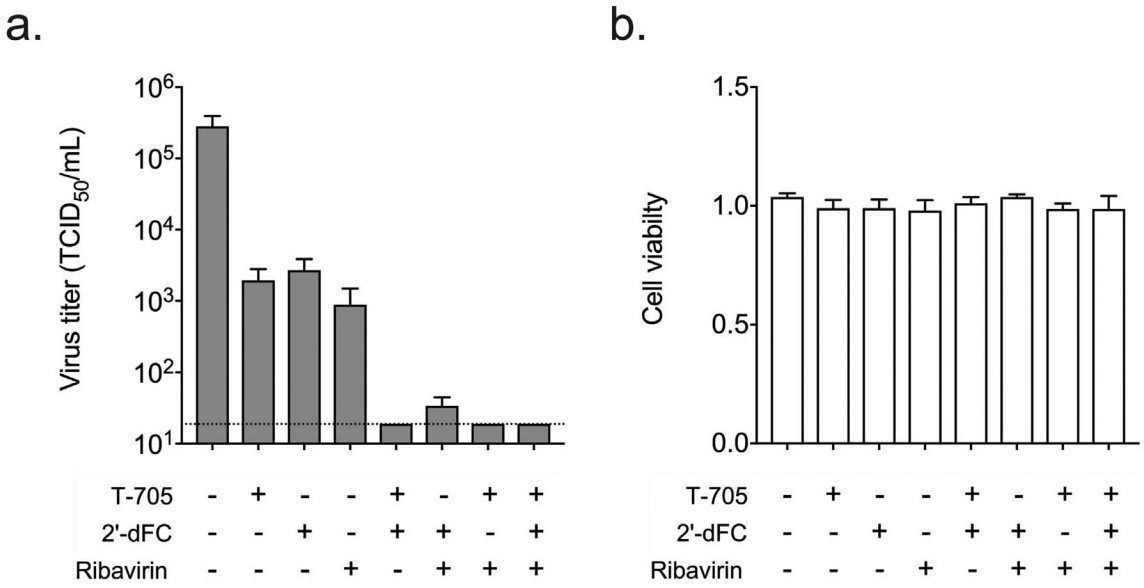

Fig. 5. Confirmatory counter-screening of maximum synergy compound concentrations using wild-type CCHFV.

a. Huh7 cells were treated with the indicated compounds either individually or in combination at the following concentrations: T-705, 2 μM; 2′-dFC, 200 nM; ribavirin, 10 μM. Cell were infected with wild-type CCHFV at MOI 0.1, and viral titers were determined at 48 hpi. Each point represents the mean of triplicate wells, with error bars indicating standard deviation. Dotted line represents the limit of detection for this assay (1.89×10^1 $TCID_{50}$/mL). **b.** Cell viability (ATP content) was determined concurrently and normalized to ATP content in mock-treated (DMSO only) Huh7 cells.

Table 1

Compounds evaluated in the antiviral screening assay, showing the 50% effective concentrations (EC_{50}) and 50% cytotoxicity concentrations (CC_{50}) of each compound in Huh7 cells. All values are in μM; selectivity indices (SI) shown in parentheses. RdRp, RNA-dependent RNA polymerase; IMPDH, inosine monophosphate dehydrogenase.

Compound	EC_{50} (SI)		CC_{50}	Compound class
	CCHFV/ZsG	CCHFV		
Ribavirin	12.48 ± 2.61 (> 10)	5.69 (> 26)	> 150.0	Guanosine (ribonucleic) analog
T-705	1.03 ± 0.16 (> 50)	0.88 (> 57)	> 50.0	Selective RdRp inhibitor
2'-Deoxy-2'-fluorocytidine	0.061 ± 0.018 (> 820)	0.031 (> 1613)	> 50.0	Nucleoside analog
Mycophenolic acid	0.10 ± 0.01 (18)	0.19 (9)	1.78 ± 0.25	IMPDH inhibitor